Electronics and Electrical Engineering

AIMS Electronics and Electrical Engineering, 4(2): 188–199.
DOI: 10.3934/ElectrEng.2020.2.188
Received: 02 February 2020
Accepted: 18 March 2020
Published: 09 April 2020

http://www.aimspress.com/journal/ElectrEng

Review

Coherence of oscillations generated by single-electronic two-dimensional arrays of tunnel junctions

Nazim F. Habbani* **and Sharief F. Babikir**

Department of Electrical and Electronics Engineering, Faculty of Engineering, University of Khartoum, Sudan

*** Correspondence:** E-mail: nzhabbani@uofk.edu; Tel: +249912396072.

Abstract: The single-electron devices (SEDs) are novel devices based on a new operation concept and technologies, with great scaling potential that has been fabricated and is under investigation. The SEDs are based on the controllable transfer of single electrons (SEs) between small conducting electrodes. They have had already several demonstrative scientific experiments as well as enabled fabrication methods. The present work studies the coherence of signals in a two-dimensional homogeneous arrays of small tunnel junctions. The Monte-Carlo technique is used to simulate the circuit and collect the required statistics. The simulator is a hybrid simulator that uses at the beginning the Master Equation representation to compute the steady-state current through the circuit. It is shown, how the coherence of oscillations is strengthened with longer arrays structures, and that the coupled two-dimensional long arrays are having strong correlated tunnel events, when the finite frequency noise characteristics and oscillations pattern variation are addressed. The variation of both the applied voltage and the coupling capacitors is illustrated. The dependency of the transport process and distribution of time between the events on their setting parameters is shown and the coefficient of variation was calculated to clarify the results. Also, the state's transition flow is reviewed for the traverse of electrons through the arrays structure for different bias conditions.

Keywords: master equation; tunneling; Coulomb blockade; Monte-Carlo modelling; power spectral density

Abbreviations: SED: single-electron device; SE: single electron; SET: singe-electron tunneling; p.d.f: probability density function; 2D: two-dimensional; 1D: one-dimensional; IV: current-voltage

1. Introduction

The current through single-electron devices is affected by the Coulomb blockade. At low bias voltages and especially at low temperatures, these devices can enter a Coulomb blockade region, where the tunneling of electrons is blocked, giving them unique properties [1]. For instance, a tunnel junction biased by a dc current may generate single-electron tunneling (SET) oscillations with average frequency $f_0 = \langle I \rangle / e$. This effect is due to the gradual accumulation of continuous charge on the junction capacitance, followed by the sudden passage of one electron through the junction, as soon as the accumulated charge has reached a threshold level $Q_t = \pm e/2$. The discreteness of charge transfer will certainly be one of the central issues facing the emerging nano-electronics. This is why it is important to formulate the conditions under which the transport of charge through a conductor may be considered as quasi-continuous. One of the most interesting systems capable of quasi-continuous charge transfer is the one-dimensional array of small tunnel junctions [2]. The key property of such an array is that each additional electron inserted into one of its islands creates a series of gradually decreasing polarization charges, and hence may be considered as a "single-electron soliton" with a characteristic that may be much larger than one island [3]. Nowadays, there are some low-cost nanofabrication technologies producing talented results for innovative nanostructures in terms of versatility and scalability. These low-cost nanofabrication approaches, like self-assembly, colloidal lithography, soft lithography, electrochemical anodization and etching approaches, in many cases, can be combined with the conventional nanofabrication technologies such as photolithography, interference lithography, electron beam lithography and focused ion beam lithography, for a promising way of generating innovative nanostructures suitable for a broad range of applications [4]. The small capacitances and tunnel junctions that build the array structures under study need a unique nanofabrication technique that best suits their properties for high resolution and high throughput in a cost-efficient manner. There are three important reasons for studying tunneling junction arrays. Firstly, because they are the simplest structures to construct for a wide range of fabrication techniques, particularly for those lithographic techniques that are the best means for the controlled fabrication of large systems of such arrays. Secondly, multiple junction arrays could be considered as a prototype for building more complex structures, and therefore be analyzed for themselves and as a route for gaining the experience and techniques necessary to analyze more complex systems. Finally, they would be important components in any extended single electronic system, as they act analogously to controlled transmission lines or shift registers. In this work, the quality of oscillations has been investigated through the dynamic charging processes coupled by the possible instantaneous tunnel processes. For that purpose, the Monte-Carlo technique has been used to trace the events and provide a platform to collect the data required to assess the quality of the resulting oscillations by computing the distribution of time between tunnel events and then calculating the frequency-dependent power spectral density of the resulting oscillations for the signal generated by the events. The modelling routine has been applied to characterize the operation of a static homogeneous two-dimensional array of small tunnel junctions.

2. Theory and model

Figure 1 shows an equivalent structure for a two-dimensional tunnel junction array under study. It consists of two series of tunneling junctions *1, 2…, i…, N*, each of capacitance C_{t1} and C_{t2}, respectively. Both of them are connected by electrodes *1, 2…, i…, N* at potential ϕ_i, and are coupled

to the ground plane via capacitances C_{01} and C_{02}. The two sets are linked together by capacitances *Cc*. The circuit is voltage biased at its two left and two right voltage terminals. The analysis is performed in a low voltage regime.

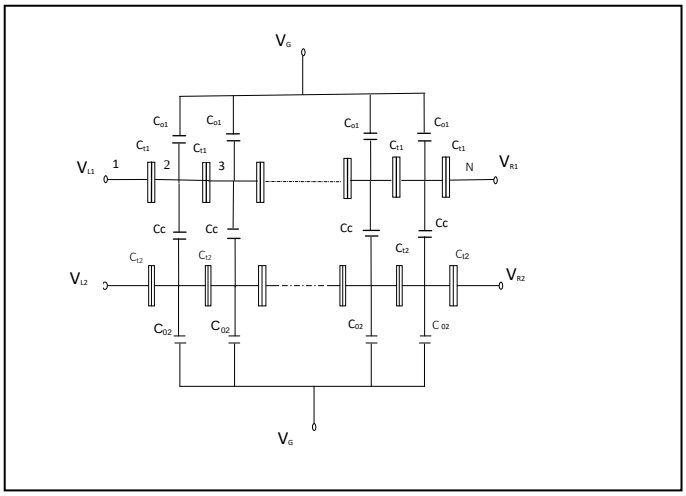

Figure 1. Circuit diagram of a homogeneous two-dimensional array of small tunnel junctions.

The potential profile created by a single excess electron located at a given node inside any of the two array legs will block other electrons from entering that part of the array. Under such conditions, the dynamic of charges transport through the two sides of the array will be dominated by a single charge tunneling in each of the array legs, from left to right, until finally exiting at the other end. At higher bias conditions, the situation changes so that it is possible that more than one electron could be found inside the structure and the time between events is a combination of different sequences. The properties of the array resulting from such sequential tunneling mode could be studied in the time domain as well as in the frequency domain. Experimentally, it is most likely that successive tunnel events may take place across non-neighboring junctions. This would require the analysis of the various state transition paths contributing to the transport process. For arrays of quantum dots biased near the threshold voltage, the transport process is well defined by a single path for conduction [5]**.**

The Monte-Carlo simulator uses the Master Equation formalism to find the steady-state current I_0 in the tunnel junction network, and then to compute the average time between successive events. This is achieved when several successive algorithms identify the list for the active states that hold the system in its steady-state. It is claimed that the steady-state and transport characteristics of single electron circuits are strongly affected by the possible states in the system and the relationships between the states [6]. The simulator then iterates "events" by repeatedly characterizing the circuit for a given set of input voltages and clocked charge positions, discovering which tunneling event will occur next and updating dependent and independent circuit parameters using charge conservation and the circuit matrix equations. Although this approach is important it is computationally expensive, especially for the larger extended systems of coupled devices. The model then divides a total time of kT_0 *(*k ~ 5 and T_0 is average time between successive events) into W slots *(*W ~ *1000).* The Monte-Carlo simulation runs so that, a total of M events crosses the junction under study *(*$M \sim 10^7$*).* The time between successive events is measured and recorded in the corresponding slots. The frequency contents resulting from the train of delta functions formed by the electrons crossing the reference tunnel junction could be computed as:

$$G(\omega) = g_i(t)\sum_i e^{-j\omega t_i} \tag{1}$$

where, $g_i(t)$ is the probability density function (p.d.f) for the time between events, evaluated as the percentage of the number of tunnel events counted in slot i to the total number of events within the time size of the slot. The probability density function is given by:

$$g_i(t) = \frac{n_i}{M\ \Delta t} \tag{2}$$

where, n_i is the number of tunnel events counted in slot i, Δt is the time size of the slot and M represents the total events. The power spectrum of the current pulses detected at the measurement point is dependent on the pattern of tunnel events and the distribution of the time between events as discussed above. The power spectral density $S(\omega)$ is estimated using the following relation [7]:

$$S(\omega) = 2eI_0 \frac{1-|G(\omega)|^2}{|1-G(\omega)|^2} \tag{3}$$

where, $I_0 = \langle I \rangle$ is the average tunneling current, $G(\omega)$ is the Fourier transform of the distribution of the time between events and e is the electron charge. For a Poisson process, the power spectral density is given by the Schottky value, $S(\omega) = 2eI_0$, which is independent of the frequency [7]. The tunneling process in single electronic circuits is a Poisson point process. The time spent at any state i depends on the transition rates from this state to any of the next states linked to this state by only one tunnel event. The probability density function of the dwelling time at that state is obtained by [5,8]:

$$f_j(t) = \Gamma_j \exp(-\Gamma_j t) \tag{4}$$

where, Γ_j represents the tunnel rates for that state.

Thus, the distribution of time between tunnel events follows a negative exponential distribution. A variable T is defined to represent the time between successive events, which estimates the dwelling time at each node. The key statistics for the time between successive events at the reference junction are given by:

$$\langle T \rangle = \sum \frac{1}{\Gamma_j} \tag{5}$$

$$\sigma^2 = \sum \frac{1}{\Gamma^2_j} \tag{6}$$

The coefficient of variation (β) or the oscillation quality factor is defined as the ratio of standard deviation divided by the mean, using Eqs (5) and (6) above:

$$\beta = \frac{\sigma}{\langle T \rangle} \tag{7}$$

The coefficient of variation is useful for comparison between data sets with different units or widely different means. It shows the extent of variability in relation to the mean of the studied data sets.

The mean $\langle T \rangle$ and the standard deviation σ for the time between successive events for the two-dimensional arrays that are having different biased conditions could be calculated statistically as:

$$\langle T \rangle = \Delta t.\sum t_i g_i(t) \tag{8}$$

$$\sigma = \sqrt{\Delta t.\sum (t_i - \langle T \rangle)^2 g_i(t)} \tag{9}$$

3. Results and discussion

The dynamics of electron transport and inter-array coupling has been studied in a homogeneous two-dimensional arrays of N small tunnel junctions. The parameters used in this model are: tunnel junction capacitance $C_t = 1.0e^{-17}$ F, ground plane coupling capacitors $C_0 = 1.0e^{-18}$ F, tunnel resistance $R_t = 100$ $k\Omega$, linking capacitors $Cc = 1.0e^{-18}$ F and the nominal applied temperature $T = 1.0e^{-07}$ K. All the junctions grounding and coupling capacitances are taken as equal to each other and to those of the corresponding ones in the other array leg. The array is attached to an ideal voltage source and the voltage applied on both of its left terminals is slightly above the threshold voltage. The analysis is performed in a low voltage regime at either of its left and right ends of the array structure, e.g. for the left-hand side of the array, with $V_{R1} = V_{R2} = 0$. The development of stable and reliable single electronic systems requires the precise design and selection of the junction capacitances (inter-capacitances), the capacitances to ground and the arrays coupling capacitances. Any slight change of such ultra-small capacitances will have remarkable consequences on the numerical simulation outcome. It can be observed from Figure 2 that, under similar operation conditions, the time between successive events leaving the array increases with increasing structure length N, because of the increase in the number of tunnel events needed to traverse longer arrays set. The reduction of the maximum values of the probability density function with increasing N indicates that the fluctuations of the time between events do increase in return. This would be clearly noticed in a linear scale plot. For relatively short arrays, the curves of the p.d.f are having single peaks, and for the later ones there is an indicator of a presence for other peaks. This will be better seen when the corresponding frequency content is plotted. The results of Figure 2 for the two-dimensional array structures match those obtained likewise for the one-dimensional array as shown in reference [9]. The figure includes a sample curve for a one-dimensional array of length $N = 40$. Under similar operation conditions, in both structures, the coherence for oscillations is improved for longer sets of arrays.

The continuing coherence of the tunnel events has also been investigated in the frequency domain using the power spectral density formulation given in Eq (3). The spectral density $S(f)$ has been computed after evaluating numerically the Fourier transforms for the time between events. Figure 3 illustrates the power spectral density for the trains of tunnel events exiting the arrays of the mentioned lengths. For comparatively short structure circuits, e.g. N = 3 or N = 7, the density starts to show a flat peak which indicates some level of correlation. The peaks become more noticeable with increasing array length and having their maximum values at approximately twice the absolute average frequency f_0. These results are in contrast to those reported for the longer arrays of the one-dimensional arrays [9], as their power spectral densities show their higher peaks around the absolute oscillation frequency. This is attributed to the difference of the transport process between them, as the two-dimensional arrays are having two legs for the conduction transitions of the electrons. The analysis for the power spectral density is in agreement with that obtained for the one-dimensional long arrays, showing that the coherence is strengthened when increasing the array length.

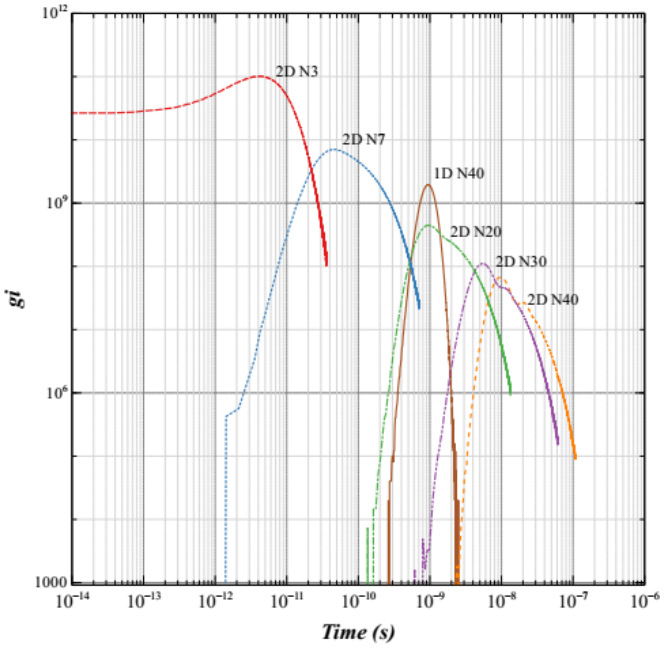

Figure 2. The p.d.f g_i across a reference tunnel junction for *2D arrays* (*N = 3, 7, 20, 30 & 40*), and a *1D array N = 40*, all are biased just above the threshold voltage. Note that log scales are used in both axes.

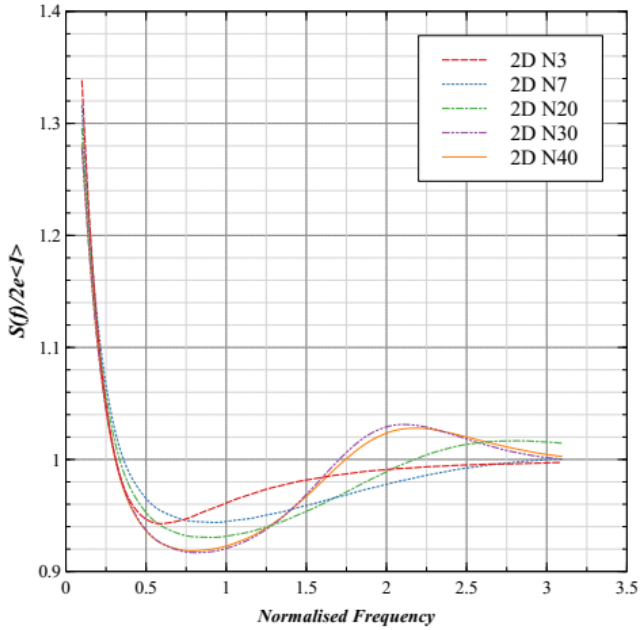

Figure 3. The power spectral density, *S(f)*, for different *2D arrays* as in Figure 2 above against the normalized frequency (f/f_0).

In Figure 4, for the same 2D array of 40 tunnel junctions circuit, the transition modes undergo different transfer processes, given the same parameters and conditions when changing the applied voltage. This shows the sensitivity of variation of biasing condition in altering the correlation between events, by increasing the number of expected events and changing the distribution of time between them.

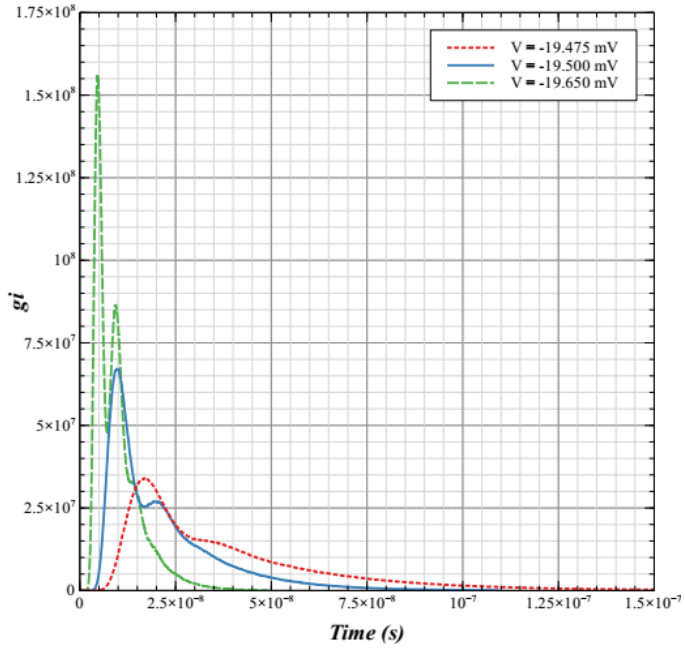

Figure 4. The probability density function gi for the array N = 40. The bias voltages applied at both V_{L1} and V_{L2} are: -19.475, -19.5 and -19.65 mV.

The power spectral density provides a clearer perception into the quality of oscillations produced by the circuit. In Figure 5, the minima peaks lie between 0.5 and 1 of the absolute frequency, and there is a presence of a first order peak for the higher bias voltage value. For all curves, there is an existence of a secondary order harmonic frequency, and the peaks become more acute as the value of the bias voltage is increased. Also, the observed modes approach the Poisson level at higher frequencies.

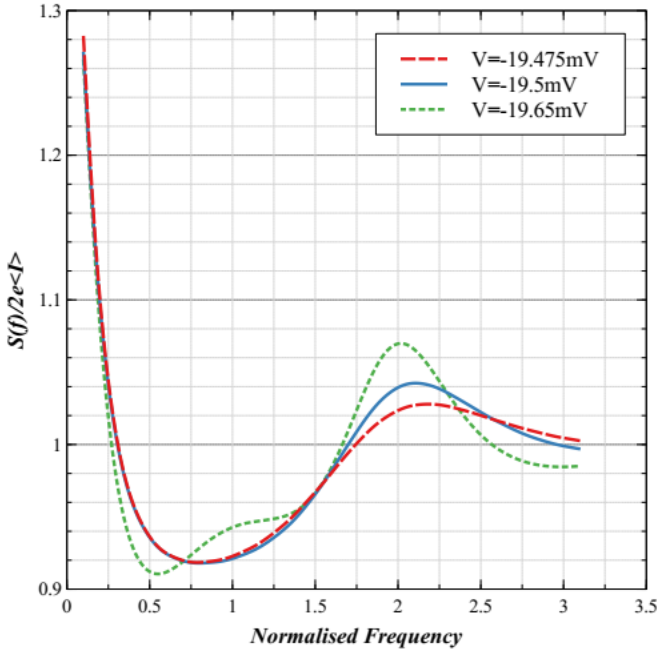

Figure 5. The power spectral density *S(f)* for *2D N = 40*, with parameters as given above in Figure 4.

Figure 6 shows the variation of the value of the linking or inter-coupling capacitors for the same 2D array structure. The electronic system is having orders of higher magnitude for the distribution of time between the events corresponding to the increase in the capacitance values. Figure 7 illustrates the probability density function using the same settings as in Figure 6. The observations noticed in Figure 6 and Figure 7 match those which have been mentioned in the corresponding Figure 4 and Figure 5, for the case of changing the bias voltage. This similarity illustrates the effect of both the bias conditions and the coupling capacitors in altering the distribution of time between the events and in terms of the transport processes of the electronic circuit.

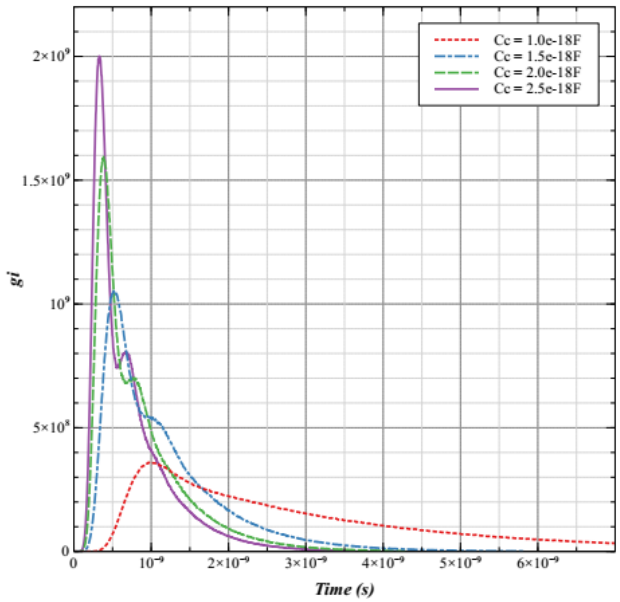

Figure 6. The distribution of time between successive events for the 2D (N = 20), for different values of linking capacitors Cc = 1.0e^{-18} F, 1.5e^{-18} F, 2.0e^{-18} F and 2.5e^{-18} F, as shown, at a fixed bias voltage.

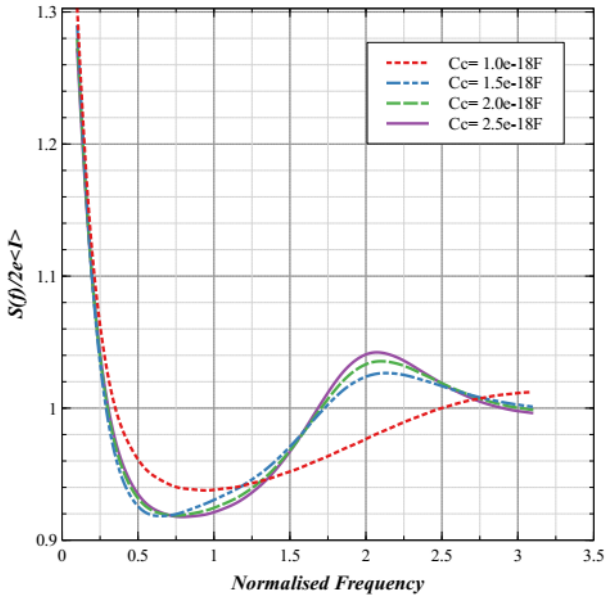

Figure 7. The power spectral density *S*(*f*) for the *2D* (*N = 20*), for same settings as in Figure 6.

In Figure 8, the oscillation quality factor (β) has been plotted against a selected set of two-dimensional arrays under the above operation conditions. For relatively short arrays *N = 7* or *N = 10*, the values are found to be 0.9379 and 0.829986, respectively. Later, the quality factor reached values around 0.7 for the rest of the set under examination. This implies that for the shorter set of arrays, the process is closely similar to that of a Poisson process or having a poor quality. These results are in agreement with those obtained for β in the one-dimensional arrays as stated in reference [9], where the quality improves with a longer set of circuits and reaches a constant value around 0.33. This is suggestive of a good quality assurance for the longer two-dimensional arrays compared to that of the one-dimensional long arrays sets, as the 2D arrays are having better variation for time between events around the means about which they occur.

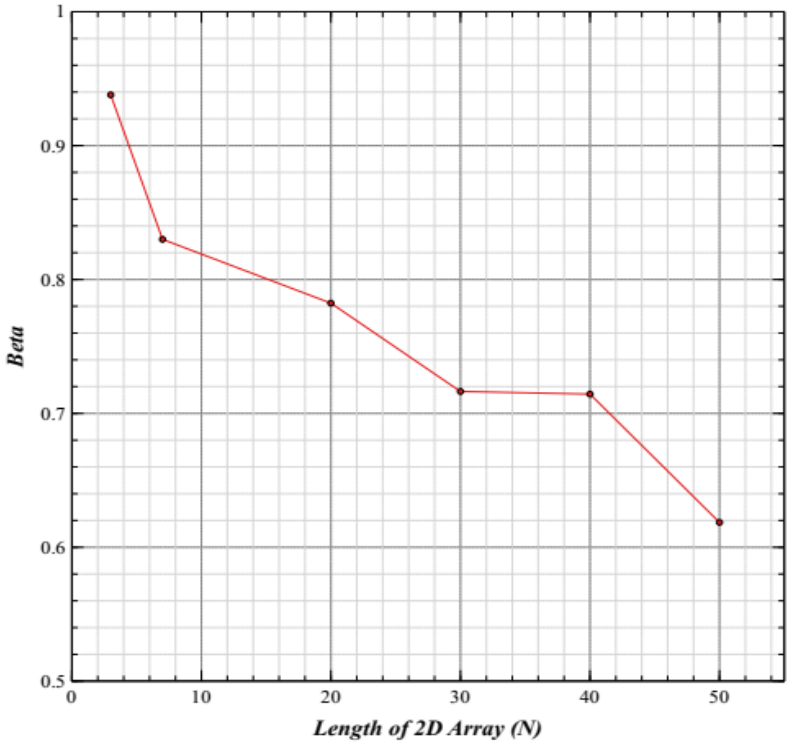

Figure 8. The coefficient of variation *β* for the time between events for the *2D arrays* (*N = 3, 7, 20, 30, 40* and *50*).

Figure 9 shows the quality factor β for the 2D array N = 20, for different values of bias voltage. The curve is gradually falling below unity as the bias voltage is increased; thus, the quality factor is dependent on the applied voltage to the electronic circuit.

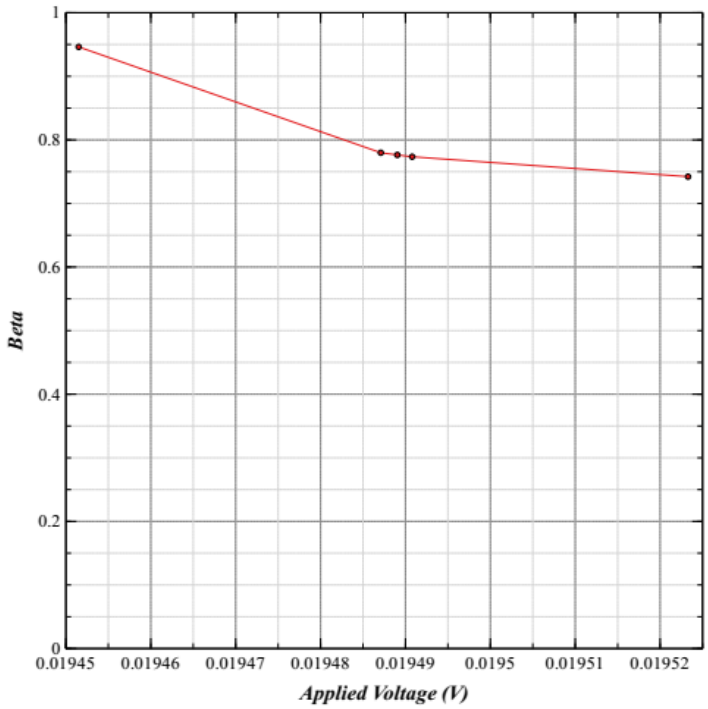

Figure 9. The coefficient of variation β for the *2D array N = 20*, for different values of bias voltage.

Table 1. Some of the state's transitions for a 2D array of tunnel junctions (*N = 20)* biased just above threshold voltage.

States	Nodes	First Array Leg	Second Array Leg
	[1->2]:		
0	* . . . . . * . . . . . *		
1	* e . . . . . * . . . . . *		
	[22->23]:		
0	* . . . . . * . . . . . *		
2	* . . . . . * e . . . . . *		
	[2->3]:		
1	* e . . . . . * . . . . . *		
3	* . e . . . . . * . . . . . *		
	[23->24]:		
2	* . . . . . * e . . . . . *		
4	* . . . . . * . e . . . . . *		
	[3->4]:		
3	* . e . . . . . * . . . . . *		
5	* . . e . . . . . * . . . . . *		
	[24->25]:		
4	* . . . . . * . e . . . . . *		
6	* . . . . . * . . e . . . . . *		

For voltages above the threshold voltage (V_{th}), the conductance process of a two-dimensional array (N = 20) goes through 41 states. There are two separate electrons within each of the array legs attached at the same time and both of them travelling in one direction from the left node towards the right node. Some of the state's transitions are shown in Table 1. The electron enters from the left point and travels from one node to the other towards the right node until it finally exits at the end of the right electrode of the structure. The presence of the single electron in any of the array legs completely blocks other electrons from entering as it is theoretically stated. Transition starts from node 1->2 in the first leg for transition state 0 to 1, and from node 22->23 in the other leg for transition state 0 to 2, which both happen at the same time. The transition then continues from node 2->3 in first leg and 23->24 in the other leg, for states 2->3 and 2->4, respectively, …etc.

When the bias is increased, another conduction path will be possible, as there is an increase in the total active states and the tunnelling events. This condition allows another electron to enter when the first one reaches the last junction. In the latter case, the second electron can progress towards the end of the array. This conduction takes place in both array legs with the same pattern. It is expected that there will be a noticeable change in the IV characteristic for the structure caused by the change in the number of states and events contributing to the conduction process.

4. Conclusion

In summary, the study of the two-dimensional array of quantum dots, shows that the relative linewidth of oscillations decreases with increasing array length. The structure is dramatically affected by the change in the bias conditions or the linking capacitors, as they change the modes of operation of the array structure and the transport through the array. The oscillations are completely messy by shot noise for arrays that are shorter than an array of 7 junctions. Without using the coupling capacitors to link the two junction tunnel arrays, the arrays operate as totally independent of each other. Comparison against experimental data for one-dimensional array confirms the similarity in operation, such as the enhancement of the coherence for the longer array structures. The two-dimensional arrays are having higher quality factors than that of the one-dimensional arrays. There is an important feature, which is the threshold voltage that is used for selecting the optimum bias values for a better operation of the two-dimensional array electronic circuits as well as for their quality of oscillation.

Conflict of interest

The authors declare that there is no conflict of interest in this manuscript.

References

1. Averin D and Likharev K (1986) Coulomb blockade of single-electron tunneling, and coherent oscillations in small tunnel junctions. *Journal of Low Temperature Physics* 62: 345–373.
2. Matsuoka KA and Likharev KK (1998) Shot noise of single-electron tunneling in one dimensional arrays. *Phys Rev B* 57: 15613–15622.
3. Hoekstra J (2009) Introduction to Nanoelectronic Single-Electron Circuit Design. Pan Stanford Publishing Pte. Ltd.

4. Santos A, Deen MJ and Marsal LF (2015) Low-cost fabrication technologies for nanostructures: state- of-the-art and potential. *Nanotechnology* 26: 042001.
5. Babiker S (2011) Shot Noise in Single Electron Tunneling Systems: a Semi-classical Model. *IEEE T Nanotechnol* 10: 1191–1195.
6. Babiker S, Naeem R and Bedri A (2011) Algorithms for the Static and Dynamic Simulation of Single-Electron Tunnelling Circuits. submitted for publication in (Journal) IET Circuits, Devices and Systems, 2011.
7. Lindner B (2006) Superposition of many independent spike trains is generally not a Poisson process. *Phys Rev E* 73: 022901.
8. Babiker SF, Bedri A (2011) Analysis of Single Electron Tunnelling Oscillations in Long Arrays of Tunnel Junctions. 6th International Conference: Sciences of Electronic, Technologies of Information and Telecommunications, Tunisia.
9. Babikir S, Alhassan ASA, Elhag NAA (2018) Coherence of Oscillations Generated by Single Electronic Circuits. International Conference on Communication, Control, Computing and Electronics Engineering (ICCCCEE), Sudan.

AIMS Press